Supplementary Information (SI) for Soft Matter.
This journal is © The Royal Society of Chemistry 2025

Supporting Information

Characterizing dynamic heterogeneities during nanogel degradation

Zafrin Ferdous Mira[1], Vaibhav Palkar[1], Olga Kuksenok[1,*]

[1]Department of Materials Science and Engineering, Clemson University, Clemson, South Carolina 29634, United States

[*]: okuksen@clemson.edu

S1. Additional details of the modeling approach and simulation parameters

Within the DPD framework, the dissipative and random contributions are defined as[1] $\boldsymbol{F}_{ij}^{D} = -\gamma\omega^{D}(r_{ij})(\boldsymbol{e}_{ij}\cdot\boldsymbol{v}_{ij})\boldsymbol{e}_{ij}$, and $\boldsymbol{F}_{ij}^{R} = \sigma\omega^{R}(r_{ij})\zeta_{ij}\overline{\Delta t}^{-1/2}\boldsymbol{e}_{ij}$, respectively, where $\boldsymbol{v}_{ij} = \boldsymbol{v}_i - \boldsymbol{v}_j$ is the relative velocity, $\overline{\Delta t}$ is the simulation time step, ζ_{ij} is a symmetric Gaussian distributed random variable with unit variance and zero mean, and coefficients γ and σ define the strengths of the respective interactions. To satisfy the fluctuation-dissipation theorem, the following conditions are imposed [1]: $\omega^{D}(r_{ij}) = (\omega^{R}(r_{ij}))^2$, and $\sigma^2 = 2\gamma k_B T/m$, where k_B is the Boltzmann constant, T is temperature, and m is a mass of the bead. We use the common choice of the weight function as[1] $\omega^{R}(r_{ij}) = (1 - r_{ij}/r_c)$. We set the mass of a bead to unity in reduced DPD units, $\gamma = 4.5$, and the beads number density to three[1].

For the harmonic bond potential, which is applied between the bonded beads, U_b, we set a spring constant[2, 3] $K_b = 10^3$ reduced units and an equilibrium bond distance as $r_0 = 0.7$ reduced units. An additional mSRP repulsive force acting between the pseudo beads located at the centers of the bonds separated by a distance $d_{ij} = |\boldsymbol{d}_{ij}|$ is introduced as[4]

$$\boldsymbol{F}_{ij}^{mSRP} = b_{ij}\left(1 - \frac{d_{ij}}{r_c^{mSRP}}\right)\boldsymbol{e}_{ij}^{s}, \quad (1)$$

provided that the distance between the centers of the bonds is below mSRP cut-off distance, r_c^{mSRP} , ($d_{ij} \leq r_c^{mSRP}$), and zero otherwise. In eq. (1), $\boldsymbol{e}_{ij}^{s} = \frac{\boldsymbol{d}_{ij}}{|d_{ij}|}$, and the parameters are set to[4] $b_{ij} = 80$ reduced units and r_c^{mSRP} is 0.80 reduced units; it had been shown that these values effectively minimize bonds crossing[3, 4].

The simulation parameters corresponding to cases A-G characterized in this work are provided in Table S1 below. We follow the procedure detailed in our recent work[2] to construct a spherical gel particle with the set number of beads between the centers of two bonded precursors, N_x. The initial structure of the nanogel is created by crosslinking four-arm precursors with the initial bond length set at 0.28. The number of unit cell replicas in x, y and z directions is 8×8×8 in cases A-E, 10×10×10 in case F, and 6×6×6 in case G, respectively. To create a spherical nanoparticle, a spherical shape is cut out from the cubic block initially created by the unit cells using the radius factor[2] of 0.77 with respect to the final radius of the sphere. The number of water beads added to the simulation box is calculated by subtracting the number of nanogel beads for each case from the total number of beads that are needed to keep chosen bead number density of three within the simulation box size defined in Table S1. Periodic boundary conditions are applied in all simulations. The nanogels are equilibrated prior to the degradation simulations. Five trajectories at selected timesteps during the equilibration simulation (at time steps $2\times10^5, 4\times10^5, 6\times10^5, 8\times10^5, 10^6$) are

chosen as initial configurations for the degradation simulations in each of the cases and are referred to as simulation runs r1,r2,r3,r4, and r5, respectively. The degradation simulations are run for Case A ((r1-r4)-10^7, r5-13×10^6), Case B((r1-r5)-10^7), Case C((r1-r4)-10^7, r5-14×10^6), Case D ((r1-r5)-10^7), Case E (r1, r2, r3, r5)-12×10^6, r4-14×10^6), Case F((r1, r3, r5)-12×10^6, (r2, r4)-14×10^6) and for Case G((r1-r5)-10^7) time steps. The simulation timestep is set as $\overline{\Delta t} = 0.02$ reduced units of time, τ. The reaction time step during which the random numbers are generated for the degradable bonds, τ_r, is taken ten times larger than the DPD time step[5-7], $\tau_r = 10\overline{\Delta t}$. Finally, reduced units of time, τ , can be related to the dimensional value via matching diffusion coefficient of water beads to known diffusion coefficient of water as[8] $\tau \approx 88$ ps.

Table S1. Simulation parameters for hydrogel particles and affinity between polymer and solvent in cases A-G characterized in this study.

Case #	# of junction*	# of end groups	# of degradable bonds	Box size	# of polymer beads	Total # of beads	N_x	a_{ij}
Case A	943	3772	1680	60×60×60	12259	648000	6	79.5
Case B	943	3772	1680	60×60×60	12259	648000	6	82.0
Case C	943	3772	1680	60×60×60	12259	648000	6	85.0
Case D	943	3772	1680	60×60×60	12259	648000	6	90.0
Case E	943	3772	1680	35×35×35	12259	128625	6	79.5
Case F	1911	7644	3520	60×60×60	17199	648000	4	79.5
Case G	417	1668	708	60×60×60	8757	648000	10	79.5

*# of junction = # of precursors

S2. Supporting figures characterizing simulation results

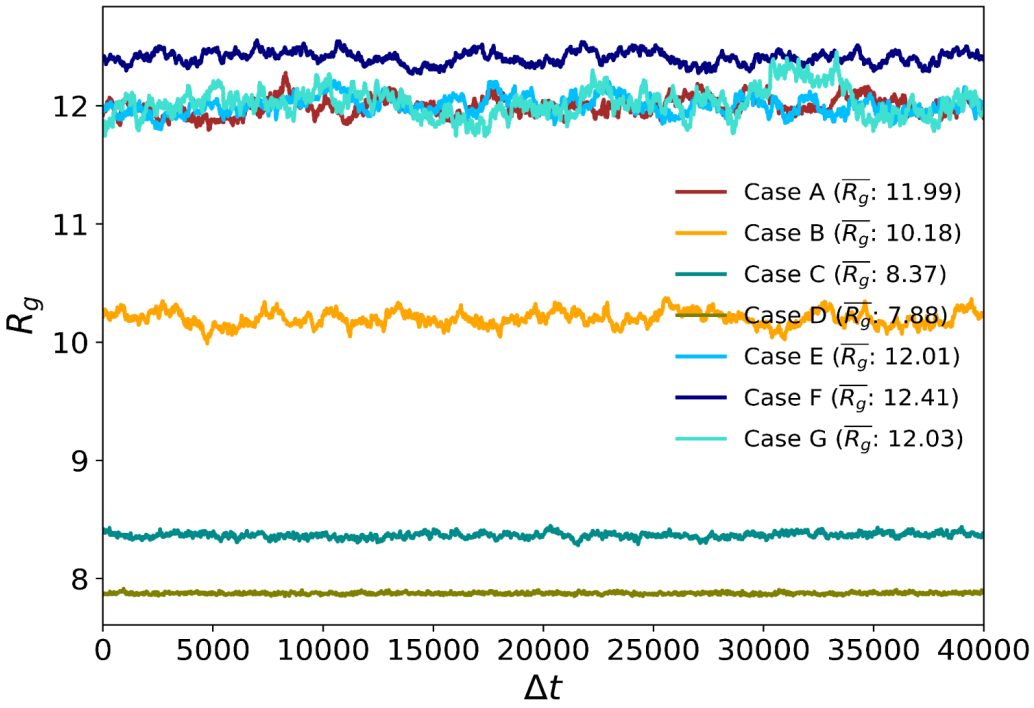

Figure S1. Radius of gyration, R_g, for equilibrated nanogels for cases A-G as marked. Herein, zero time corresponds to the systems pre-equilibrated in solvents of the corresponding quality (as defined in Table S1) for 10^6 timesteps from the initial configuration as shown in Figure 1a. For each case, an average radius of gyration, $\overline{R}_g$, is provided in legend in reduced DPD units of $\tilde{r}_c \approx 0.65$nm.

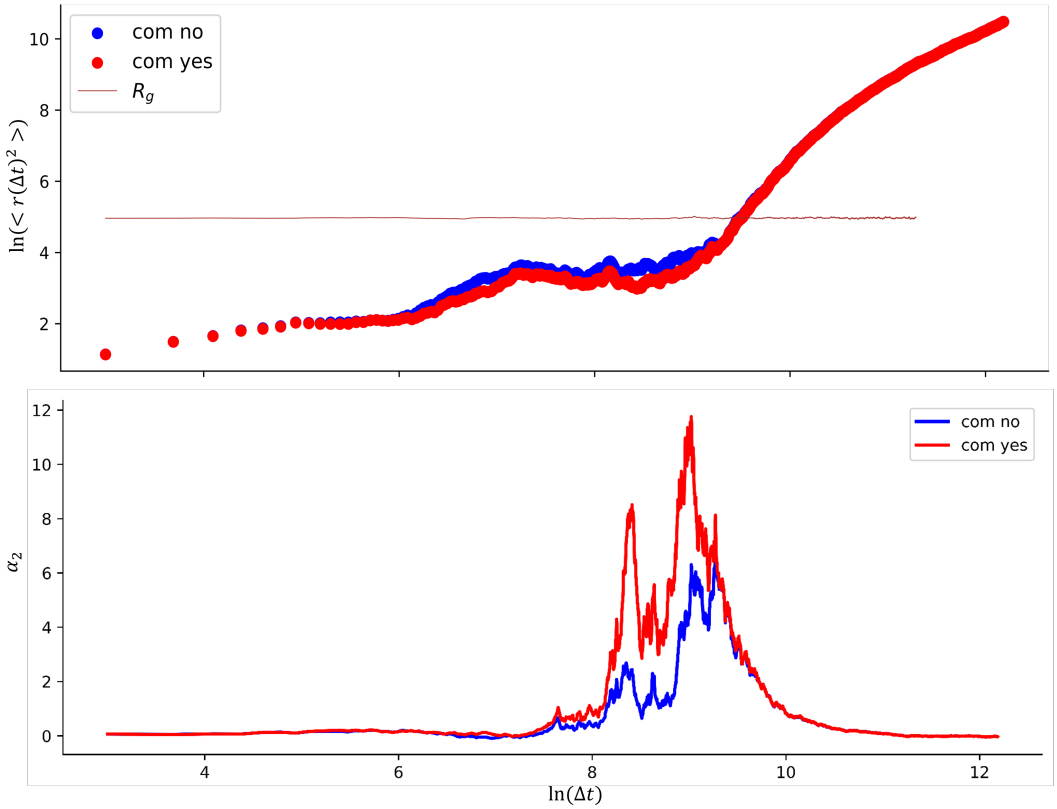

Figure S2. Time evolution of the mean squared displacement, $< r(\Delta t)^2 >$, and non-Gaussian parameter α_2, calculated with (in red) and without (in blue) accounting for the drift of the center-of-mass of the polymer system, respectively. Dotted line in the top image corresponds to $\bar{R}_g{}^2$, where $\bar{R}_g$ is an average radius of gyration in equilibrium (prior to degradation) for the same case A (see Fig. S1). The blue curves are the same as shown in Figure 2 of the main text. The plots are for the reactive beads during nanogel degradation.

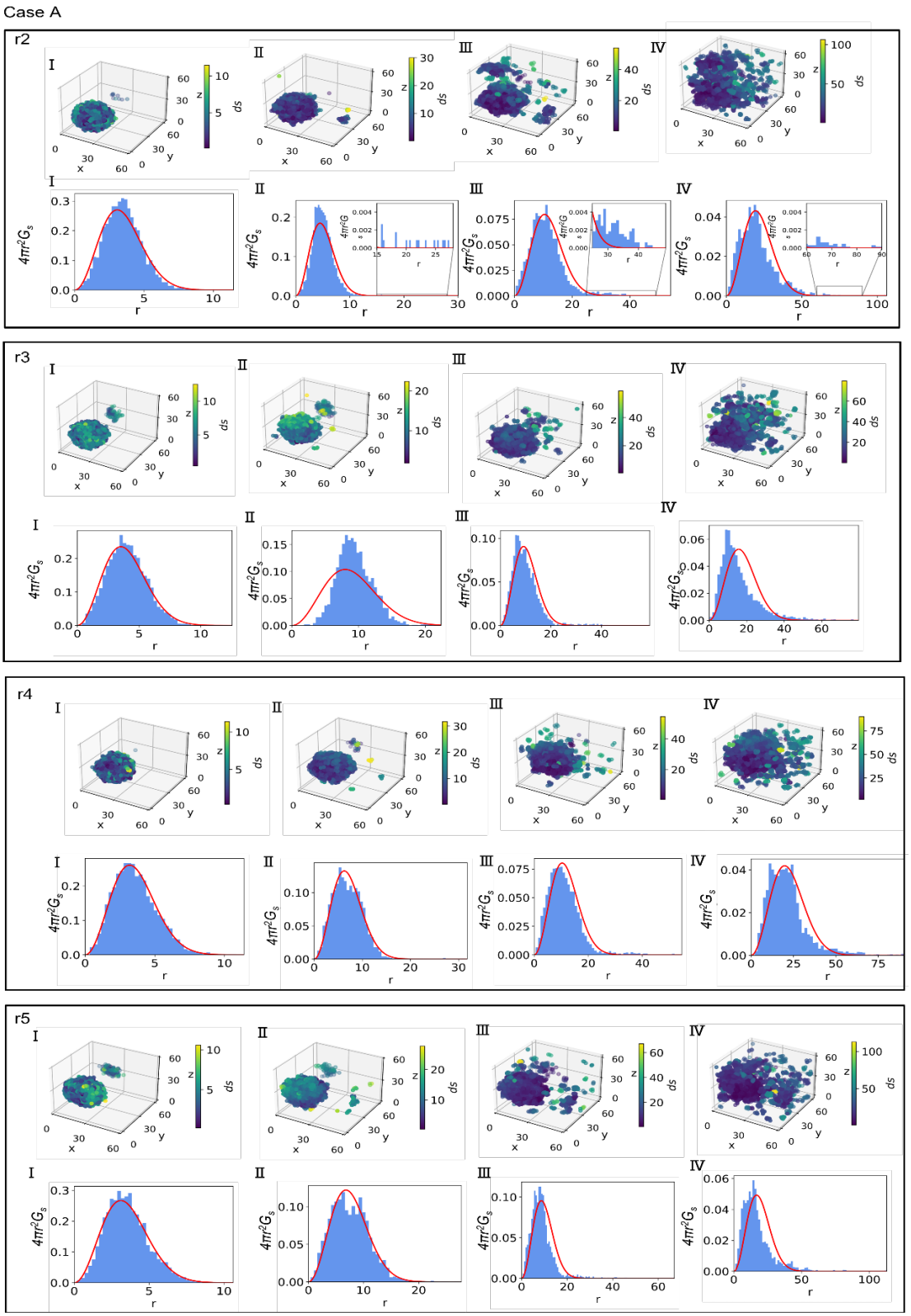

Figure S3. Heat map of displacements of reactive beads and probability density of the displacements of reactive beads during the degradation of nanogel at the time instants marked (I-IV) in Figure 2 (r2-r5).

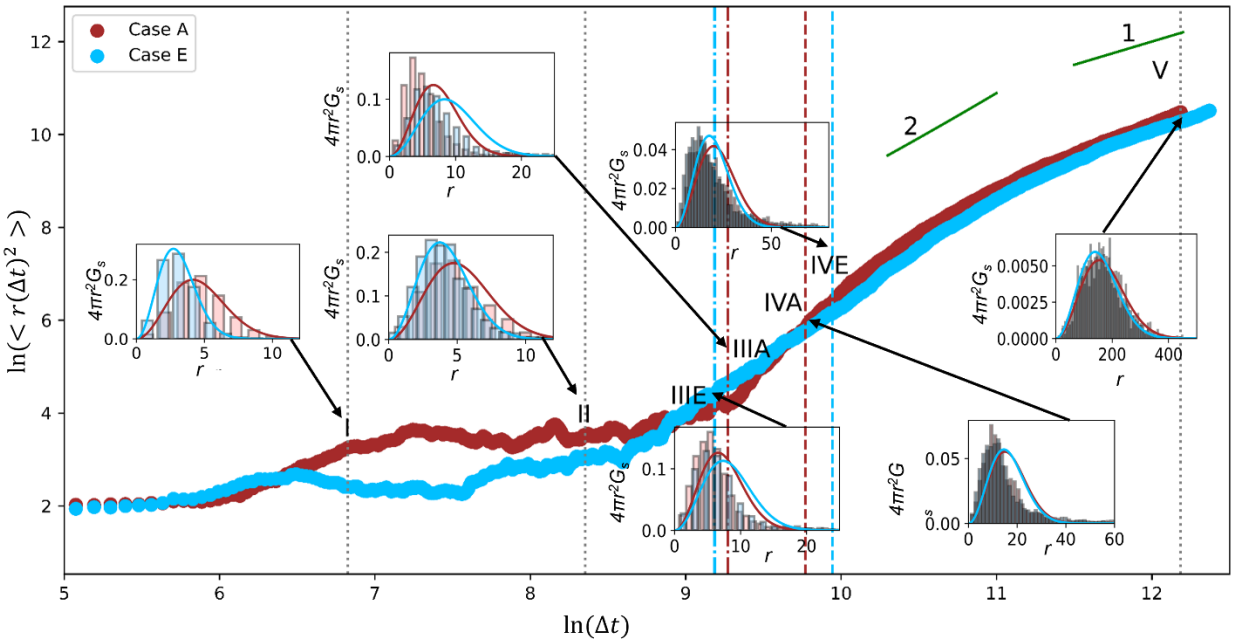

Figure S4. Mean Squared Displacement (msd) of the reactive beads as a function of time from the onset of nanogel degradation. The insets show probability density of the displacements of reactive beads at different time instants as marked; simulation data for cases A and E are shown as bar plots in red and blue, respectively. Gaussian distribution is also shown in the insets (red and blue curves, respectively).

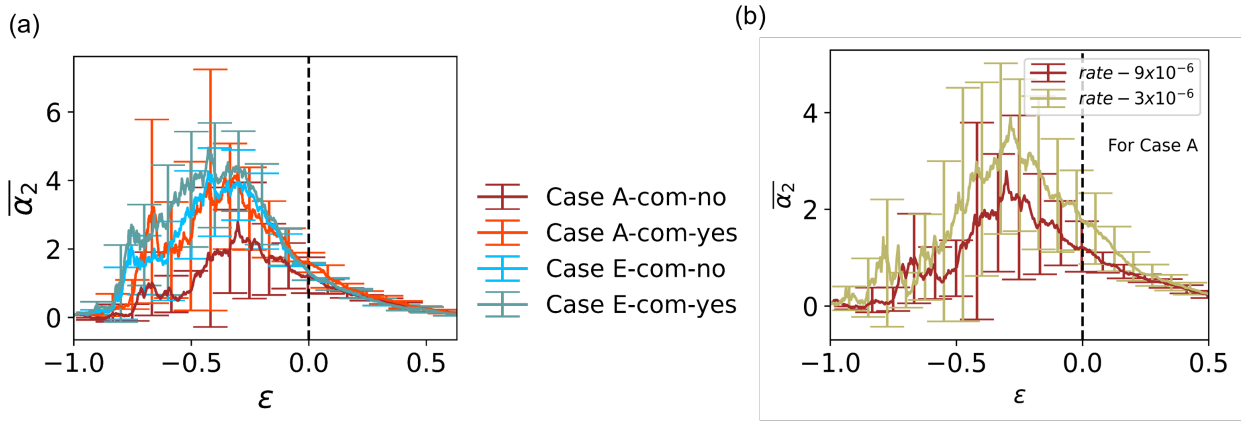

Figure S5. Averaged non-Gaussian parameter as a function of the relative extent of reaction, ϵ, for cases A and E in (a) and for two different probabilities of bonds breaking for case A in (b): red curve corresponds to $P = 9 \cdot 10^{-6}$ (reference value, same as red curve in (a)), and yellow curve corresponds to $P = 3 \cdot 10^{-6}$. In (a), we provide average values of α_2 calculated for both cases A and E without and with subtracting drift of the center-of-mass of the reactive beads before the displacement of each bead is calculated (data marked com-no and com-yes, respectively). In all the cases, the averages are taken over five independent simulation runs using the displacements of all reactive beads.

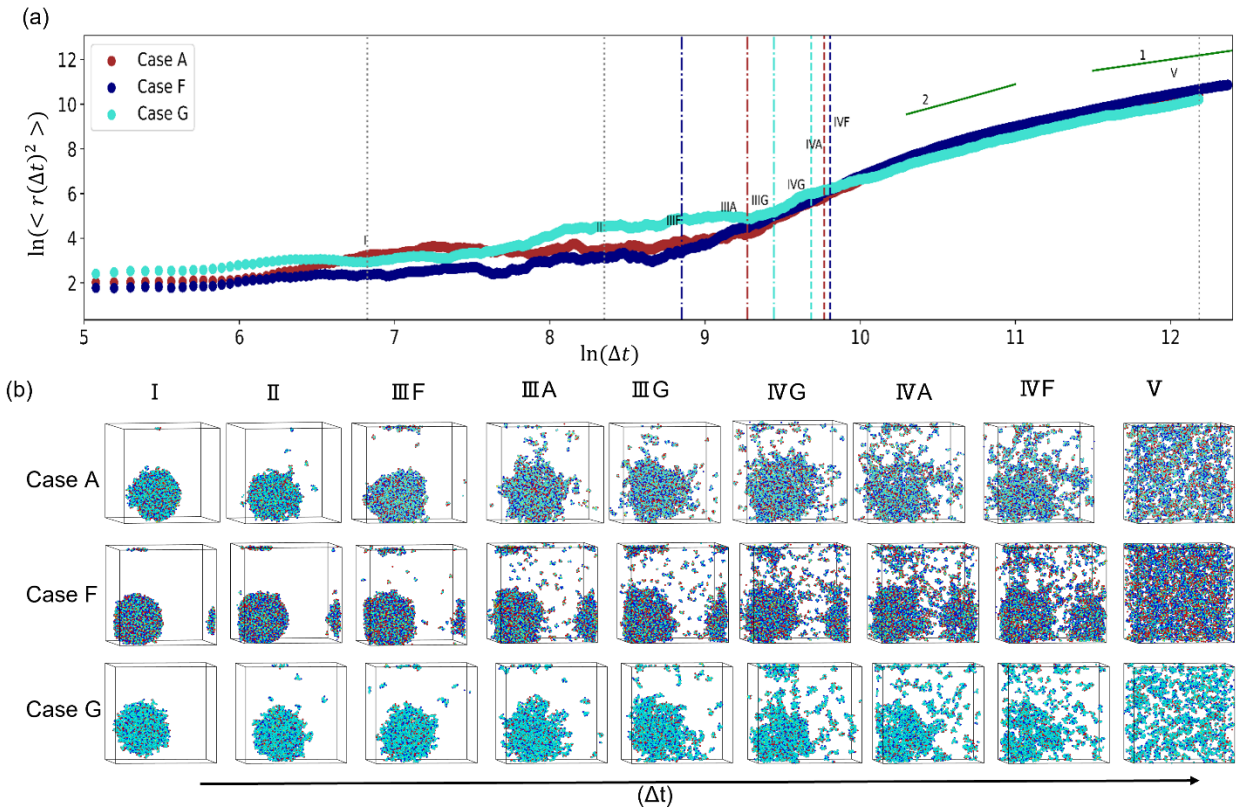

Figure S6. (a) Mean squared displacement of reactive beads as a function of time during hydrogel degradation; brown, navy, and turquoise curves correspond to cases A, F, and G, respectively. Simulation snapshots at the time instances marked by I, II, III(A, F, G), IV(A, F, G) and V are shown. (b) Simulation snapshots during the hydrogel degradation in cases A, F and G at the time instances marked in (a).

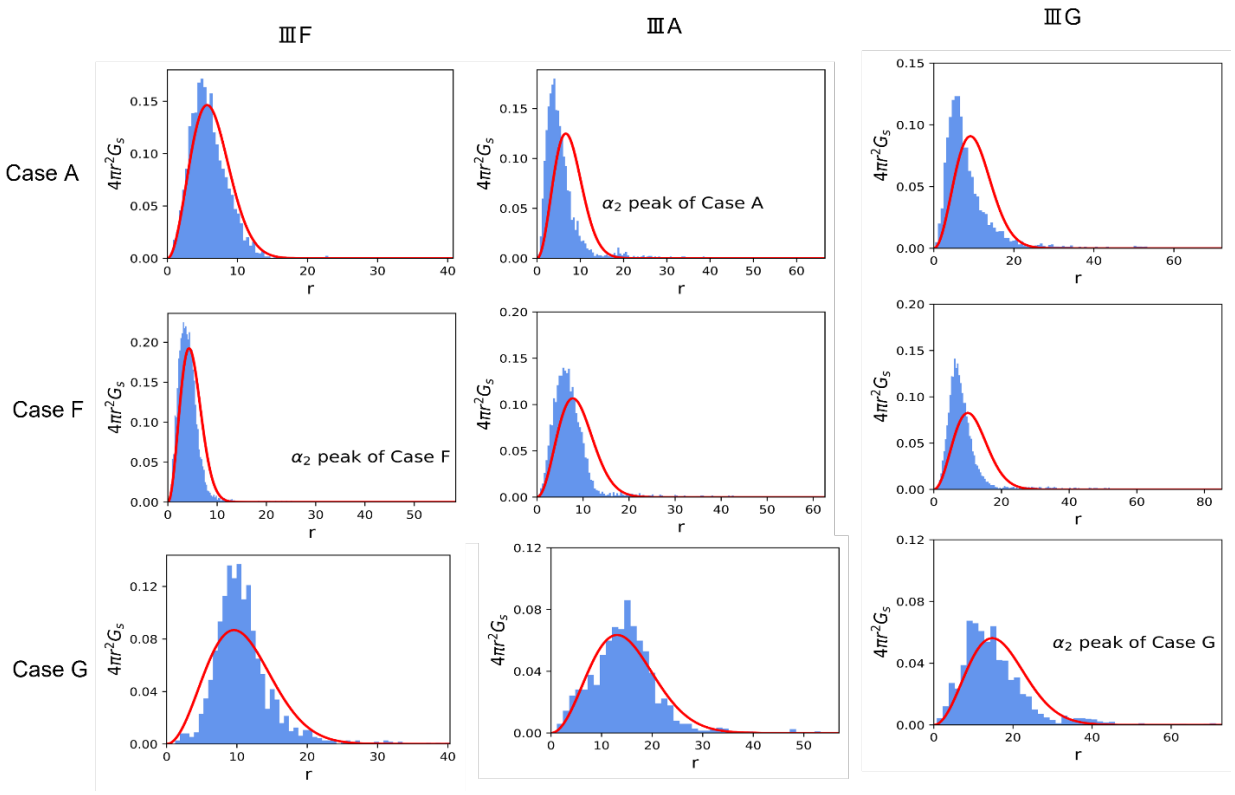

Figure S7. Probability density of the displacements of reactive beads during the hydrogel degradation for Cases A, F and G at the time instances marked by IIIF, IIIA, IIG in Figure S6. Gaussian distributions are shown in red.

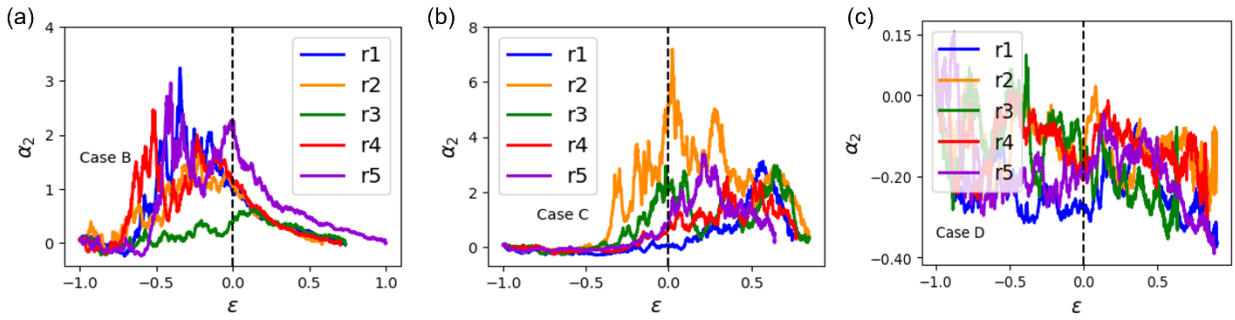

Figure S8. Non-Gaussian parameter, α_2 of reactive beads during nanogel degradation as a function of the relative extent of degradation, ϵ, for five individual simulation runs (r1-r5) for cases B, C and D in (a), (b), and (c), respectively.

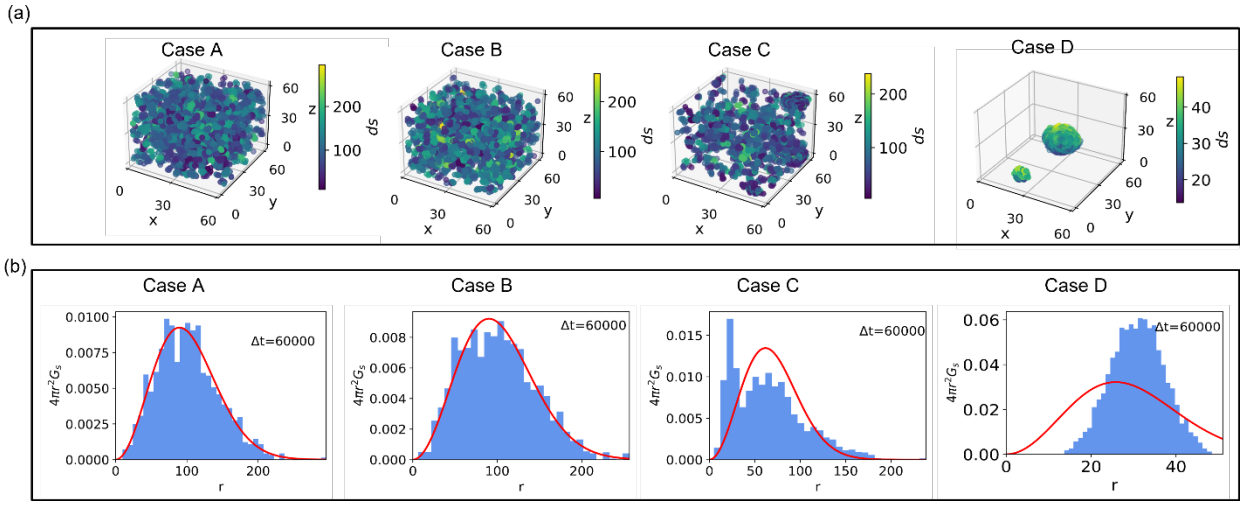

Figure S9. (a) Heat map of displacements of reactive end groups. (b) Probability density of the displacements of reactive beads at the same time instants of (a); bar plots represent simulation data, and red curves correspond to Gaussian distribution. The plots are for reactive beads of seed r1 for a fully degraded system starting from a fully degraded position. From left to right is, respectively, Case A, B, C and D.

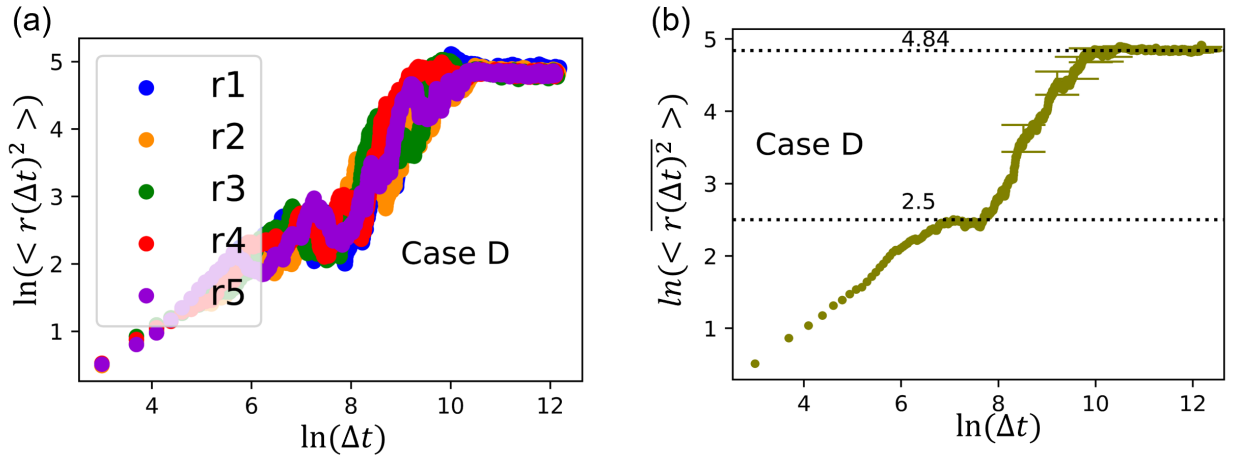

Figure S10. (a) Mean-squared displacement as a function of time for five simulations in Case D. Herein, the effect of the drift of the center-of-mass of the reactive beads is subtracted out before the displacement of each bead is calculated (com=yes option in compute msd command in LAMMPS). The averaged mean-squared displacement as a function of time for (a) is shown in (b). The dotted lines mark average plateau values of $ln < (r\Delta t)^2 >$ in (b), with the lower plateau corresponding to the characteristic length scale of ≈ 3.5 and the upper plateau corresponding to ≈ 11.25 reduced DPD units (so that $\ln(3.5^2) \approx 2.5$ and $\ln(11.25^2) \approx 4.84$ as marked by the dotted lines, respectively)

References

1. Groot, R. D.; Warren, P. B., Dissipative particle dynamics: Bridging the gap between atomistic and mesoscopic simulation. *J. Chem. Phys.* **1997,** *107* (11), 4423-4435.
2. Palkar, V.; Thakar, D.; Kuksenok, O., Nanogel degradation at soft interfaces and in bulk: tracking shape changes and interfacial spreading. *Macromolecules* **2023,** *56* (4), 1289-1302.
3. Palkar, V.; Kuksenok, O., Controlling Degradation and Erosion of Polymer Networks: Insights from Mesoscale Modeling. *J. Phys. Chem. B* **2022,** *126* (1), 336-346.
4. Sirk, T. W.; Slizoberg, Y. R.; Brennan, J. K.; Lisal, M.; Andzelm, J. W., An enhanced entangled polymer model for dissipative particle dynamics. *J. Chem. Phys.* **2012,** *136* (13), 11.
5. Liu, H.; Li, M.; Lu, Z. Y.; Zhang, Z. G.; Sun, C. C., Influence of Surface-Initiated Polymerization Rate and Initiator Density on the Properties of Polymer Brushes. *Macromolecules* **2009,** *42* (7), 2863-2872.
6. Yong, X.; Kuksenok, O.; Matyjaszewski, K.; Balazs, A. C., Harnessing Interfacially-Active Nanorods to Regenerate Severed Polymer Gels. *Nano Letters* **2013,** *13* (12), 6269-6274.
7. Yong, X.; Kuksenok, O.; Balazs, A. C., Modeling free radical polymerization using dissipative particle dynamics. *Polymer* **2015,** *72*, 217-225.
8. Groot, R. D.; Rabone, K. L., Mesoscopic Simulation of Cell Membrane Damage, Morphology Change and Rupture by Nonionic Surfactants. *Biophys. J.* **2001,** *81* (2), 725-736.